Laser-Heating Effect on Raman Spectra of Individual Suspended Single-Walled Carbon Nanotubes

Yingying Zhang,[†] Hyungbin Son,[‡] Jin Zhang,*[,†] Jing Kong,*[,‡] and Zhongfan Liu*[,†]

Centre for Nanoscale Science and Technology (CNST), Beijing National Laboratory for Molecular Sciences (BNLMS), State Key Laboratory for Structural Chemistry of Unstable and Stable Species, Key Laboratory for the Physics and Chemistry of Nanodevices, College of Chemistry and Molecular Engineering, Peking University, Beijing 100871, P.R. China, and Department of Electrical Engineering and Computer Science, Massachusetts Institute of Technology, Cambridge, Massachusetts 02139

Received: September 14, 2006; In Final Form: November 10, 2006

We studied the Raman spectra of 21 individual suspended single-walled carbon nanotubes (SWNTs) using different excitation laser powers. The results indicate that the laser-heating effect is more significant for suspended SWNT than nanotubes sitting on a substrate. The spectral variations of these individual SWNTs induced by different laser power shed new light on the temperature dependence of Raman spectra and electronic properties of SWNTs. By analyzing the frequency downshift of each nanotube induced by increased laser power, the temperature coefficient of radial breathing mode (RBM) frequency ω_{RBM} is supposed to be diameter- and chirality-dependent, whereas that of the G-band frequency $\omega_G{}^+$ is not. The behaviors of full width at half-maximum (fwhm) and intensity ratio between anti-Stokes and Stokes spectra (I_{AS}/I_S) of RBM with increasing laser power reflected the temperature increase and the consequent variation in the electronic density of states (DOS) of SWNT. The variation of resonance intensity with laser power showed interesting dependence on $E_{ii} > E_{laser}$ or $E_{ii} < E_{laser}$, suggesting downshift of E_{ii} with increased temperature, which offers the possibility of utilizing the optical/thermal response of SWNT to modulate the electronic property of nanotubes.

Introduction

Resonance Raman spectroscopy (RRS) has been demonstrated to be an effective and nondestructive means to characterize the electronic and vibrational properties of single-walled carbon nanotubes (SWNTs).[1,2] Suspended SWNTs, being free of environmental perturbations, have been shown to have enhanced Raman signal, decreased line width, and richer spectral information compared with nanotubes on substrates.[3] Although the heating effect induced by the laser power (with power density ~ 1 mW/μm^2) of the Raman measurement is generally neglectable for SWNTs on substrates, it is expected to be notable for suspended ones because of its remarkable optical absorption ability[4−6] and lack of effective "heating sinking".[7] As more and more attention has been devoted to the resonance Raman spectra of suspended SWNTs, it is important to investigate how and to what extent the laser-heating effect will influence the Raman spectra and the electronic properties of these suspended SWNTs.

On the other hand, the temperature dependence of Raman spectra of SWNTs has been investigated in the past several years.[8−14] The position of Raman peaks[8−11,14] and the electronic transition energies (E_{ii})[12,13,15,16] of SWNTs are found to shift with temperature. However, most of the experimental works[8,10−12,14] are done on bulk samples in which nanotubes with a wide distribution of diameters and different chirality are present. The resulting spectra generally show a superposition of Raman scattering from all active nanotubes. Even for a certain nanotube, as the interactions between nanotube and its surroundings are sensitive to temperature, the results cannot present the pure temperature effect on nanotube. To study the temperature influence on Raman spectra of nanotubes, individual suspended nanotubes are the ideal choice. In this paper, ultralong and partially suspended SWNTs have been prepared on trench-contained substrate. The Raman spectra of 21 individual suspended SWNTs have been collected using micro-Raman spectroscopy with tuned laser power. The result reveals the remarkable laser-heating effect on suspended SWNTs. Moreover, as done on individual and suspended SWNTs, it sheds new light on the pure temperature effect on Raman spectra of SWNTs and suggests the diameter and chirality dependence of temperature coefficients of ω_{RBM}.

Experimental Section

1. Preparation and Characterization of Suspended SWNTs. The substrates used in this study are silicon wafers with a 300-nm-thick oxide layer on the surface, which contains trenches of 1∼80 μm wide and 300-nm deep. SWNTs were grown on the trench-containing substrate using ethanol chemical vapor deposition (CVD) and $FeCl_3$ catalyst.[17] Parallel, long carbon nanotubes, which span across the trenches, can be routinely prepared. Figure 1a is a typical scanning electron microscope (SEM) image of the sample used in this study. The distance between the parallel nanotubes is generally above 10 μm. SWNTs can be freely suspended over 3-μm-wide trenches (300-nm deep), as has been confirmed by SEM and atomic force microscope (AFM), shown in Figure 1c and d. For wider trenches, SWNTs will come into contact with the bottom of the trench (shown in Figure 1b). All the Raman spectra of suspended SWNTs in this study were taken from nanotubes across 3-μm-wide trench.

* Authors to whom correspondence should be addressed.
[†] Peking University.
[‡] Massachusetts Institute of Technology.

10.1021/jp066016e CCC: $37.00
Published on Web 01/17/2007

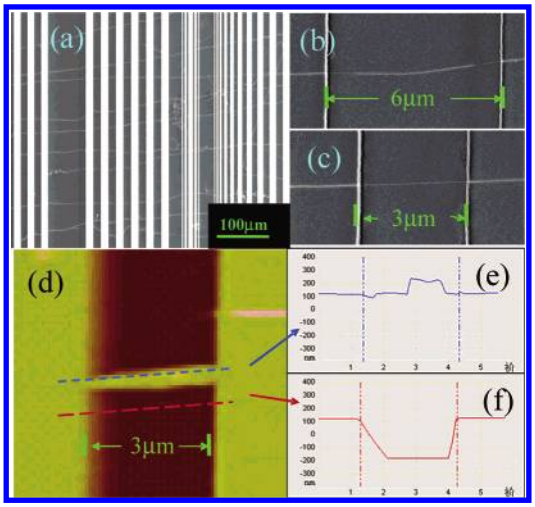

Figure 1. (a) SEM image showing oriented long SWNTs on trench-containing substrate (lighter color indicates the trench); the depth of the trenches is 300 nm. (b) SEM image showing an individual SWNT touching the bottom of a 6-μm-wide trench. (c) SEM image showing an individual SWNT freely suspended over a 3-μm-wide trench. (d) Tapping-mode AFM image shows SWNT suspended over a 3-μm-wide trench. (e) AFM section profile along the suspended nanotube across the trench showing the nanotube being suspended over trench. The irregular section profile is induced by the instability of suspended nanotube under AFM tip. (f) AFM section profile across the trench without the nanotube.

2. Raman Spectra Measurement. Resonant Raman spectroscopy (Renishaw microprobe RM1000) with a 632.8-nm (1.96 eV) He−Ne laser was used in this study. The excitation spot size is about 1 μm^2 using a 50× objective lens. We used four laser power levels in this study, which are 0.043, 0.13, 0.31, and 1.07 mW, as measured by a power meter at the sample stage. With the help of SEM image and trench features on the substrate, Raman spectra of a specific nanotube can be readily carried out. We found resonant SWNTs by scanning the laser spot along a trench and then collected their Raman spectra with various laser power levels at selected spots along the nanotube. Both RBM and G-mode Raman spectra of 21 SWNTs were taken with the light polarized parallel along the nanotube axis. All the spectra were fitted by Lorentzian line shape. Although the resolution of the spectrometer is about 1 cm^{-1}, the peak position stability in our measurement is much better than 1 cm^{-1} as observed experimentally, so we believe the peak shifts below 1 cm^{-1} are meaningful and are considered in our discussion.

Results and Discussion

1. Raman Spectra Variation of Suspended SWNT with Increasing Laser Power. We examined the Raman spectra variation of suspended SWNTs when the laser power is tuned from 0.043 mW to 1.07 mW. A typical result is shown in Figure 2, which demonstrates a downshift of 3.6 cm^{-1} in RBM frequency (ω_{RBM}) and 2.6 cm^{-1} in G^+ frequency ($\omega_G{}^+$). Along with the frequency downshift, full width at half-maximum (fwhm) and intensity ratio of anti-Stokes to Stokes (I_{AS}/I_S) of RBM also showed an obvious change. This result shows that, for suspended SWNTs, there is an obvious laser-heating effect. Repeated experiments show that the spectral variations induced by laser heating are reversible, which means there is no structural damage to the SWNT. The spectra of nanotubes lying on substrate were also examined for comparison, but no change was observed when tuning the laser power in the same range, which indicates the heating effect for nanotubes on substrate is not observable, consistent with previous reports.[18] Additionally, to confirm the origin of the Raman shifting, we used a programmable hot stage to study the Raman spectra behaviors with temperature. Although only several nanotubes which are in excellent Raman resonance among the 21 nanotubes are suitable for that experiment because of Raman intensity shrinkage induced by the sealed hot stage, it convinced us that the above-mentioned Raman spectra variations of suspended nanotubes are induced by the laser-heating effect (see Supporting Information).

We believe the remarkable laser absorption ability[4−6,19] and the poor heating dissipation of suspended SWNTs[5,7] are responsible for the observed heating effect. It has been demonstrated that SWNTs can be heated by light illumination, even to a temperature as high as its ignition point.[5,6,20] Furthermore, it is expected that the optical absorption will be enhanced when the laser energy (E_{laser}) is in resonance with one of the E_{ii} in the density of state (DOS) of an SWNT. Generally, for nanotubes on a substrate, the absorption from a

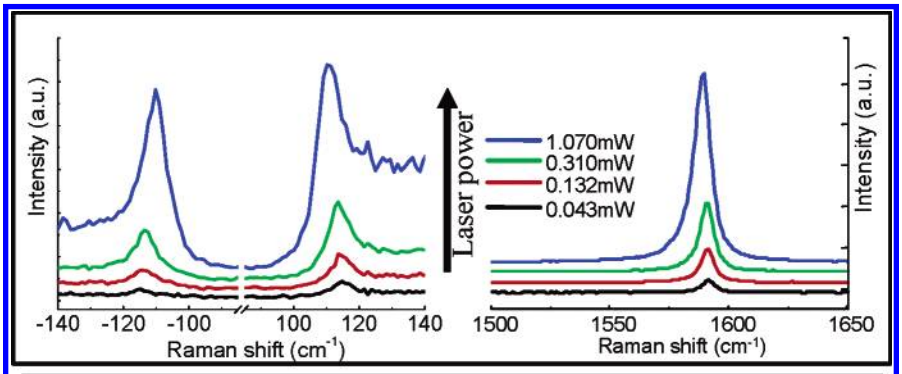

Power (mW)	ω_{RBM}(cm^{-1})	FWHM(cm^{-1})	I_{AS}/I_S	$\omega_G{}^+$(cm^{-1})
0.043	115.2	6.8	0.46	1592.2/-
0.132	115.0	6.8	0.58	1591.7/1587.9
0.310	114.3	7.6	0.68	1591.0/1585.1
1.070	111.6	9.1	0.96	1589.6/1586.7

Figure 2. (Upper): Raman spectra of an individual suspended SWNT obtained with four different laser power levels. (Bottom table): The frequency, fwhm, I_{AS}/I_S of RBM and the frequency of G-mode fitted by Lorentzian line shape. Each row corresponds to results obtained by a fixed laser power. The frequency of RBM and G^+ feature downshifts, the fwhm is broadened, and the I_{AS}/I_S increases with increased laser power.

TABLE 1: Summarized Data for 21 SWNTs Investigated in this Study, Each Row Corresponds to Data Taken from the Same SWNT[a]

no.	ω_{RBM} (cm^{-1})	$\Delta\omega_{RBM}$ (cm^{-1})	I_{AS}/I_S (1)	I_{AS}/I_S (2)	fwhm (1) (cm^{-1})	fwhm (2) (cm^{-1})	$\Delta\omega_G^+$ (cm^{-1})	metallicity	$E_{ii} > E_{laser}$ or $E_{ii} < E_{la\ ser}$
1	282.5	−0.4	0.12	0.12	2.4	2.8	−1.7	S	<
2	243.7	−0.1	1.23	1.26	5.6	6.8	−	S	>
3	201.7	−0.6	0.10	0.10	7	7	−	M	<
4	200.4	0	0.13	0.13	3.8	3.8	−	M	<
5	193.7	−0.9	0.13	0.14	4.7	4.7	−1.3	M	<
6	187.4	0	0.13	0.17	2.9	3.1	−1.1	M	<
7	169.8	−0.2	0.40	0.36	2.8	3.2	−2.0	M	<
8	167.6	0	0.80	0.97	3.1	3.7	−1.0	M	>
9	167.5	0	0.92	0.85	3.1	3.3	−0.8	M	>
10	159.9	0	1.0	1.0	4.0	4.8	−0.2	S	>
11	157.5	−1.8	0.96	0.85	8.2	11	−0.3	S	>
12	151.8	0	0.46	0.58	3.3	3.7	−1.0	S	<
13	148.4	−0.5	1.1	1.1	3.6	4.6	−2.5	S	>
14	144.0	−0.2	0.82	0.74	4.1	3.9	−1.4	S	>
15	141.3	−0.4	0.25	0.35	3.8	5.0	−1.8	S	<
16	139.6	0	0.44	0.44	4.0	5.1	−0.8	S	<
17	129.9	−2.6	1.7	1.9	5.4	6.5	−1.5	S	>
18	122.3	−0.5	0.35	0.43	3.5	4.1	−0.6	S	<
19	117.0	−1.8	0.7	0.8	4.9	4.3	−1.3	S	>
20	115.8	−1.1	1.55	1.55	4.6	4.9	−0.9	S	>
21	115.2	−3.6	0.46	0.95	6.8	9.1	−2.6	S	<

[a] ω_{RBM} indicates frequency of RBM collected with low laser power with no heating effect. $\Delta\omega_{RBM}$ and $\Delta\omega_G^+$ indicate the shift of ω_{RBM} and ω_G^+, when tuning laser power from low to the largest (1.07 mW). I_{AS}/I_S is the intensity ratio of anti-Stokes to Stokes of RBM. fwhm is the full width at half-maximum of RBM. The tag (1) indicates signals collected with low laser power and (2) indicates signals collected with high laser power. "−" means the data is not available because of weak peak. In the column "metallicity", "M" denotes metallic nanotubes and "S" denotes semiconducting nanotubes. The relationship between E_{ii} (in Raman resonance) and E_{laser} is shown in the last column.

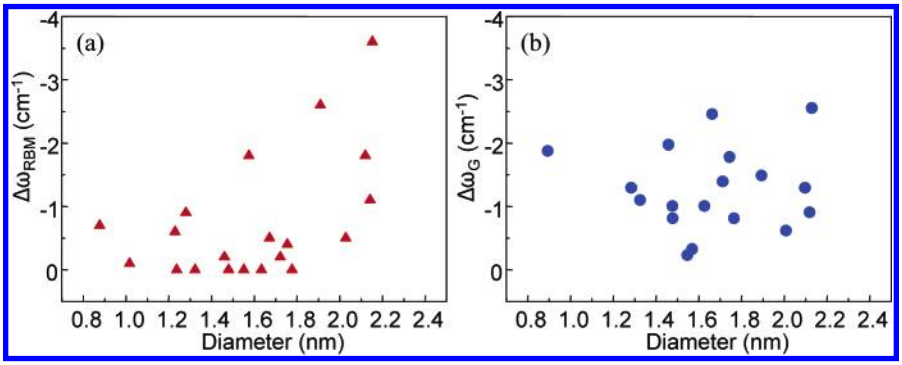

Figure 3. The dependence of $\Delta\omega_{RBM}$ (a) and $\Delta\omega_G^+$ (b) on diameter of SWNTs. $\Delta\omega_{RBM}$ shows increasing trend with increased diameter, in contrast to $\Delta\omega_G^+$.

laser with moderate power density (such as 1 mW/1 μm^2) will not induce a temperature increase, because of the effective heat sinking of the underlying substrate.[7] However, for suspended SWNTs, there is no substrate as heat sinking, and the heat may dissipate through three routes: thermal radiation, thermal conduction of air, and thermal conduction of nanotube. Because of the nanoscale dimension of SWNTs[21] and low thermal conductivity of air (~0.03 $Wm^{-1}\ K^{-1}$), the main route of heat dissipation should be from the thermal conduction of nanotube. Even the thermal conductivity of an individual SWNT is nearly 3500 $Wm^{-1}\ K^{-1}$ at room temperature,[22] and the heat in suspended SWNT still cannot be efficiently conducted away because of its nanometer cross section and finally results in temperature increase of nanotube.

2. Downshift in Frequency of RBM and G-Band Induced by Laser Heating Effect. The shifts in ω_{RBM} ($\Delta\omega_{RBM}$) and in ω_G^+ ($\Delta\omega_G^+$) (G^+ refers to the higher frequency component of G-band spectra) of each nanotube induced by increased laser power are analyzed and summarized in Table 1. We plot the diameter (d_t, calculated by $d_t = 248/\omega_{RBM}$,[1] using ω_{RBM} value with low laser power with no heating effect) dependence of $\Delta\omega_{RBM}$ and $\Delta\omega_G^+$ in Figure 3a and Figure 3b. SWNTs with larger diameters tend to exhibit a larger $\Delta\omega_{RBM}$, while no large $\Delta\omega_{RBM}$ occurs for small diameter nanotubes, as seen in Figure 3a. In contrast to $\Delta\omega_{RBM}$, $\Delta\omega_G^+$ shows no clear diameter dependence, as shown in Figure 3b.

The origin of the frequency downshifts in Raman spectra of SWNTs with increasing temperature has been proposed previously, including thermal expansion[8,14,20,23] and softening of C−C bonds.[11,24] The former corresponds to the change in the interatomic distance induced by thermal expansion of the crystal and the latter relates to the softening of modulus because of increase in temperature without an anharmonic contribution.[25,26] The latter one explains our results better: First, thermal expansion of SWNT is predicted to be extremely small by molecular dynamics simulation[11] and it only has a minor effect on the frequency of RBM, which cannot interpret the observed 3.6 cm^{-1} downshift of ω_{RBM} in our study. Moreover, smaller diameter tubes are expected to have a larger thermal expansion,[11] which is in conflict with the diameter dependence of $\Delta\omega_{RBM}$ and $\Delta\omega_G^+$ shown in Figure 3.

The different diameter dependence of $\Delta\omega_{RBM}$ and $\Delta\omega_G^+$ can be understood by the following: Here, a temperature coefficient ($d\omega/dT$) is used to denote the shifting extent of Raman peaks

with temperature. Because the laser absorption ability of nanotubes depends on the energy separation $|E_{laser} - E_{ii}|$ (the E_{ii} is in resonance with E_{laser}),[5] the extent of heating has no direct relationship with diameter. The observed different diameter dependences of Raman modes should derive from the characteristics of these Raman modes. In other words, they suggest different structure dependences of $d\omega_{RBM}/dT$ and $d\omega_G^+/dT$. As the G^+-feature is associated with C−C vibrations along the nanotube axis, ω_G^+ is essentially independent of diameter,[2] so it is conceivable that $d\omega_G^+/dT$ shows no diameter dependence. In contrast to G^+, RBM corresponds to vibration of carbon atoms in radial directions, thus, ω_{RBM} is closely dependent on tube diameter.[1,2] As SWNT can be envisioned as rolled-up graphite layer, the strain energy due to the curvature of graphite layer is inversely proportional to the diameter of nanotube. Therefore, the softening of C−C bond will be smaller for smaller diameter nanotubes[24] and larger $d\omega_{RBM}/dT$ is expected for nanotubes with large diameter.

As for the fact that also some large diameter nanotubes showed small $\Delta\omega_{RBM}$, we suspect that this indicates the chirality dependence of $d\omega_{RBM}/dT$, but to our best knowledge, there are no theoretical predictions on this issue currently. However, we notice that diverse temperature coefficients of ω_{RBM}, such as -0.0045 cm^{-1}/K for 182 cm^{-1},[11] -0.0097 cm^{-1}/K for 197 cm^{-1},[9] and -0.009 cm^{-1}/K for 264 cm^{-1},[11] have been reported by different investigators. It was also mentioned[16] that no change was observed for 268 cm^{-1} in the temperature range of -160 to 300 °C. Combining these facts and the results of 21 SWNTs in our study, we suppose that, besides diameter dependence, the $d\omega_{RBM}/dT$ may also be related to the chiral angle, which is an interesting issue needing further investigation.

3. Variation in the Line Width of RBM. The variations in the line width of RBM are examined for each individual SWNT with increased laser power. As shown in Table 1, most of these SWNTs show a slight broadening in fwhm, with the exception of no. 3−5 showing little change and no. 14 and no. 19 showing a slight narrowing.

To understand the above behaviors, both factors related to temperature-dependent phonon−phonon/electron−phonon scattering process and resonance condition of Raman scattering are considered. The first one will lead to line width broadening with increasing temperature,[10] which is consistent with most of the results shown in Table 1. Besides, it is well-known that the resonance Raman process of SWNT is closely related to the resonance condition ($|E_{laser} - E_{ii}|$).[1] It is an important factor determining the line width, which relates to the lifetime of intermediate states.[10] Departures from the resonance condition result in the broadening of line width. Better energy coherence will give rise to narrower line width. Since E_{ii} is temperature-dependent, $|E_{laser} - E_{ii}|$ can become larger or smaller with increased temperature, which may lead to line width broadening or narrowing. Therefore, we believe the fwhm variations in this study are due to the combinations of the above two factors and the narrowing in fwhm indicates the E_{ii} variations with increased temperature.

4. I_{AS}/I_S of RBM and Resonance Intensity Evolvement. The variations in I_{AS}/I_S of RBM for each individual SWNT are listed in Table 1. With increasing laser power, nine SWNTs showed an increase in I_{AS}/I_S value, while four SWNTs showed a decrease and the left eight SWNTs showed no observable change.

The I_{AS}/I_S variations also can be understood by the increase of temperature and the consequent changes in electron DOS in SWNT. The experimentally measured value of I_{AS}/I_S [I_{AS}/I_S (exp.)] can be given by the following:[13]

$$\frac{I_{AS}}{I_S}(\text{exp.}) = \frac{|(E_{laser} - E_{ii} - i\Gamma)(E_{laser} + E_{ph} - E_{ii} - i\Gamma)|^2}{|(E_{laser} - E_{ii} - i\Gamma)(E_{laser} - E_{ph} - E_{ii} - i\Gamma)|^2} \exp\left(-\frac{E_{ph}}{k_B T}\right) \quad (1)$$

where E_{laser} and E_{ii} are the same meaning as formerly defined, E_{ph} is the phonon energy ($\hbar\omega_{RBM}$), Γ is the inverse lifetime of the intermediate electronic state, k_B is the Boltzmann constant, and T is the temperature of SWNT. The second term of eq 1 will increase with temperature. However, if E_{ii} and Γ are temperature-dependent, the overall behavior can be complicated, I_{AS}/I_S (exp.) may increase or decrease with increased temperature.

The E_{ii} shift induced by temperature change has been reported by several researchers,[9,10,12−16] however, as for the shift direction of E_{ii} with temperature, there have been different opinions. The temperature-dependence of E_{ii} was investigated on nanotubes dispersed in solution,[13] and it was reported that E_{ii} shifts in two directions depending on $\nu = (n - m) \bmod 3 = 1$ or 2, which was attributed to enhanced trigonal distortion. However, several recent works[10,15,16] argued the downshift of E_{ii} with increased temperature in view of electron−phonon coupling. Another work[14] suspected the upshift of E_{ii} with temperature, which is induced by thermal expansion.

To find evidence for temperature-induced upshift or downshift of E_{ii}, we examined the resonance intensity variations with laser power, and the results suggest the downshift of E_{ii} for all the nanotubes with increased temperature. The resonance intensity is closely dependent on the resonance condition $|E_{laser} - E_{ii}|$. Smaller $|E_{laser} - E_{ii}|$ results in stronger resonance. Intensity of Stokes RBM comes from both incident (E_{laser}) photon and scattered ($E_{laser} - E_{ph}$) photon. According to eq 1, if $E_{ii} > E_{laser}$, the value of I_{AS}/I_S (exp.) will be larger than the thermal factor $\exp(-\hbar\omega_{RBM}/k_BT)$, and if $E_{ii} < E_{laser}$, I_{AS}/I_S (exp.) will be smaller than $\exp(-\hbar\omega_{RBM}/k_BT)$. By comparing I_{AS}/I_S (exp.) (with low laser power) with $\exp(-\hbar\omega_{RBM}/k_BT)$ [$T = 300$ K], the 21 SWNTs can be divided into two kinds with $E_{ii} > E_{laser}$ (10 SWNTs) and $E_{ii} < E_{laser}$ (11 SWNTs). For each nanotube, its resonance intensity variation with laser power (temperature) can be obtained by plotting its intensity normalized by its corresponding laser power level. Interestingly, among the 10 nanotubes with $E_{ii} > E_{laser}$, six of them show an increased intensity with increased laser power, three of them first show intensity increase and then show decrease, and one nanotube shows an overall intensity decease, as displayed in Figure 4a and b. Among the 11 nanotubes with $E_{ii} < E_{laser}$, seven of them show an intensity decrease with increased laser power, three of them first show intensity increase and then show decrease, and one nanotube shows an overall intensity increase as displayed in Figure 4c and d.

For nanotubes with $E_{ii} > E_{laser}$, when E_{ii} downshifts with temperature, $|E_{laser} - E_{ii}|$ becomes smaller and the resonance condition is satisfied better. This is consistent with the increased resonance intensity of the six nanotubes. Similarly, if during the E_{ii} downshift the minimum point of $|E_{laser} - E_{ii}|$ is passed, the intensity will first increase and then decrease. Additionally, the shortening of the lifetime of intermediate electron states with increased temperature, say, a larger Γ value, will result in intensity decrease, which may explain the results of SWNT no.17 (overall intensity decrease) (Figure 4b). The results of

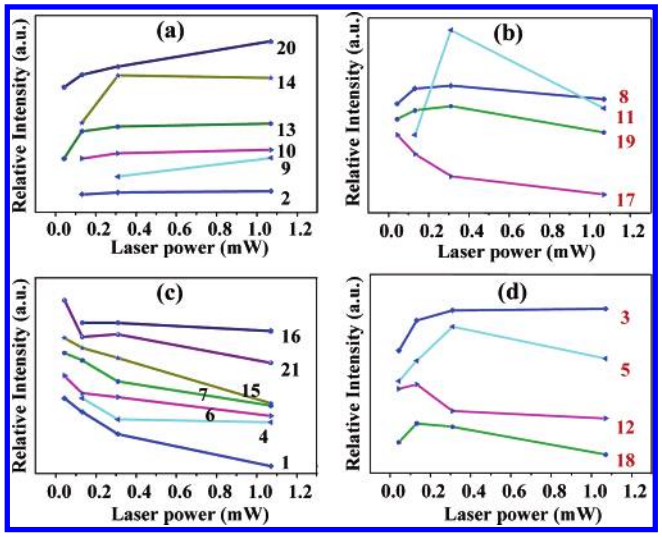

Figure 4. The variation of relative intensity of RBM with changing laser power for 21 individual SWNTs. The numbers of each SWNT are labeled beside their plot. (a, b): Plot for SWNTs with $E_{ii} > E_{laser}$; (c, d): Plot for SWNTs with $E_{ii} < E_{laser}$.

nanotubes with $E_{ii} < E_{laser}$ can be understood by a similar argument with the downshift of E_{ii} induced by increased temperature. The first increase trend shown in Figure 4d can be understood by that the downshift of E_{ii} leads to a better resonance between E_{ii} and scattered photon ($E_{laser} - E_{ph}$), although $|E_{laser} - E_{ii}|$ becomes larger.

Conclusions

The laser-heating effect on Raman spectra of SWNTs was investigated by examining Raman spectra variations of 21 individual suspended SWNTs with different laser power levels. The results indicate that the laser-heating effect is much more notable for suspended SWNTs in contrast to nanotubes sitting on substrate, which is ascribed to the good optical absorption and inefficient heat dissipation of suspended SWNTs. This suggests more attention should be paid to the potential heating effect with suspended SWNTs under investigation. Besides, it opens the possibility of using suspended SWNTs as optical−thermal devices.

The Raman spectra variations of 21 individual SWNTs with laser power shed new light on the temperature behavior of SWNTs. The frequency of RBM and G-band showed downshift with increasing laser power, which is consistent with the softening of C−C bond with temperature. On the basis of analyzing the diameter dependence of $\Delta\omega_{RBM}$ and $\Delta\omega_G^+$, $d\omega_{RBM}/dT$ is supposed to depend not only on diameter but also on chirality, while $d\omega_G^+/dT$ does not. Most of the nanotubes showed broadening in fwhm with several exceptions, which can be explained in terms of temperature-dependent electron−phonon and phonon−phonon scattering process and temperature-induced resonance condition variation. I_{AS}/I_S showed a diverse variations along laser power, resulting from the combination of increased thermal factor with the variations of E_{ii} and Γ. Moreover, the trend of resonance intensity variation with laser power showed interesting dependence on $E_{ii} > E_{laser}$ or $E_{ii} < E_{laser}$, suggesting the downshift of E_{ii} with increased temperature. This offers the possibility that utilizing the optical/thermal response of SWNT to modulate its electronic property.

Acknowledgment. This work was supported by NSFC (20573002, 20673004, 50521201), MOST (2006CB0N0701, 2006CB0N0403), and FOKYING TUNG Education Foundation (94012). H. Son and J. Kong gratefully acknowledge support from the Intel Higher Education Program.

Supporting Information Available: A description of heating experiment using a hot stage, Raman spectra of SWNT (no. 17) at different temperatures (Figure S1), and plot of its Raman peak position versus temperature (Figure S2). This material is available free of charge via the Internet at http://pubs.acs.org.

References and Notes

(1) Jorio, A.; Saito, R.; Hafner, J. H.; Lieber, C. M.; Hunter, M.; McClure, T.; Dresselhaus, G.; Dresselhaus, M. S. *Phys. Rev. Lett.* **2001**, *86*, 1118.

(2) Dresselhaus, M. S.; Dresselhaus, G.; Saito, R.; Jorio, A. *Phys. Rep.* **2005**, *409*, 47.

(3) Son, H. B.; Hori, Y.; Chou, S. G.; Nezich, D.; Samsonidze, G. G.; Dresselhaus, G.; Dresselhaus, M. S.; Barros, E. B. *Appl. Phys. Lett.* **2004**, *85*, 4744.

(4) Freitag, M.; Martin, Y.; Misewich, J. A.; Martel, R.; Avouris, P. H. *Nano Lett.* **2003**, *3*, 1067.

(5) Itkis, M. E.; Borondics, F.; Yu, A. P.; Haddon, R. C. *Science* **2006**, *312*, 413.

(6) Ajayan, P. M.; Terrones, M.; de la Guardia, A.; Huc, V.; Grobert, N.; Wei, B. Q.; Lezec, H.; Ramanath, G.; Ebbesen, T. W. *Science* **2002**, *296*, 705.

(7) Cao, H.; Wang, Q.; Wang, D. W.; Dai, H. J. *Small* **2005**, *1*, 138.

(8) Li, H. D.; Yue, K. T.; Lian, Z. L.; Zhan, Y.; Zhou, L. X.; Zhang, S. L.; Shi, Z. J.; Gu, Z. N.; Liu, B. B.; Yang, R. S.; Yang, H. B.; Zou, G. T.; Zhang, Y.; Iijima, S. *Appl. Phys. Lett.* **2000**, *76*, 2053.

(9) Zhou, Z. P.; Dou, X. Y.; Ci, L. J.; Song, L.; Liu, D. F.; Gao, Y.; Wang, J. X.; Liu, L. F.; Zhou, W. Y.; Xie, S. S.; Wan, D. Y. *J. Phys. Chem. B* **2006**, *110*, 1206.

(10) Jorio, A.; Fantini, C.; Dantas, M. S. S.; Pimenta, M. A.; Souza, A. G.; Samsonidze, G. G.; Brar, V. W.; Dresselhaus, G.; Dresselhaus, M. S.; Swan, A. K.; Unlu, M. S.; Goldberg, B. B.; Saito, R. *Phys. Rev. B* **2002**, *66*, 115411.

(11) Raravikar, N. R.; Keblinski, P.; Rao, A. M.; Dresselhaus, M. S.; Schadler, L. S.; Ajayan, P. M. *Phys. Rev. B* **2002**, *66*, 235424.

(12) Karaiskaj, D.; Engtrakul, C.; McDonald, T.; Heben, M. J.; Mascarenhas, A. *Phys. Rev. Lett.* **2006**, *96*, 106805.

(13) Fantini, C.; Jorio, A.; Souza, M.; Strano, M. S.; Dresselhaus, M. S.; Pimenta, M. A. *Phys. Rev. Lett.* **2004**, *93*, 147406.

(14) Zhang, Q.; Yang, D. J.; Wang, S. G.; Yoon, S. F.; Ahn, J. *Smart Mater. Struct.* **2006**, *15*, S1.

(15) Capaz, R. B.; Spataru, C. D.; Tangney, P.; Cohen, M. L.; Louie, S. G. *Phys. Rev. Lett.* **2005**, *94*, 036801.

(16) Cronin, S. B.; Yin, Y.; Walsh, A.; Capaz, R. B.; Stolyarov, A.; Tangney, P.; Cohen, M. L.; Louie, S. G.; Swan, A. K.; Unlu, M. S.; Goldberg, B. B.; Tinkham, M. *Phys. Rev. Lett.* **2006**, *96*, 127403.

(17) Zhang, Y. Y.; Zhang, J.; Son, H. B.; Kong, J.; Liu, Z. F. *J. Am. Chem. Soc.* **2005**, *127*, 17156.

(18) Souza, A. G.; Chou, S. G.; Samsonidze, G. G.; Dresselhaus, G.; Dresselhaus, M. S.; An, L.; Liu, J.; Swan, A. K.; Unlu, M. S.; Goldberg, B. B.; Jorio, A.; Gruneis, A.; Saito, R. *Phys. Rev. B* **2004**, *69*, 115428.

(19) Zhang, Y.; Iijima, S. *Phys. Rev. Lett.* **1999**, *82*, 3472.

(20) Huang, F. M.; Yue, K. T.; Tan, P. H.; Zhang, S. L.; Shi, Z. J.; Zhou, X. H.; Gu, Z. N. *J. Appl. Phys.* **1998**, *84*, 4022.

(21) Fujii, M.; Zhang, X.; Xie, H. Q.; Ago, H.; Takahashi, K.; Ikuta, T.; Abe, H.; Shimizu, T. *Phys. Rev. Lett.* **2005**, *95*, 065502.

(22) Pop, E.; Mann, D.; Wang, Q.; Goodson, K.; Dai, H. J. *Nano Lett.* **2006**, *6*, 96.

(23) Huong, P. V.; Cavagnat, R.; Ajayan, P. M.; Stephan, O. *Phys. Rev. B* **1995**, *51*, 10048.

(24) Ci, L. J.; Zhou, Z. P.; Song, L.; Yan, X. Q.; Liu, D. F.; Yuan, H. J.; Gao, Y.; Wang, J. X.; Liu, L. F.; Zhou, W. Y.; Wang, G.; Xie, S. S. *Appl. Phys. Lett.* **2003**, *82*, 3098.

(25) Tan, P. H.; Deng, Y. M.; Zhao, Q.; Cheng, W. C. *Appl. Phys. Lett.* **1999**, *74*, 1818.

(26) Zouboulis, E. S.; Grimsditch, M. *Phys. Rev. B* **1991**, *43*, 12490.